Colloid & Polymer Science Colloid Polym Sci 272: 400–408 (1994)

Branched non-ionic oligo-oxyethylene V-amphiphiles effect of molecular geometry on LC-phase behavior 2

K. Kratzat and H. Finkelmann

Institut für Makromolekulare Chemie, Universität Freiburg, Freiburg i. Br., Germany

Abstract: A homologous series of double-chain non-ionic surfactants with the general formula $(C_n)_2$ GE_mM, where C_n denotes an alkyl chain, G a triglyceryl, and E_mM an oligo-oxyethylene mono-methyl ether are synthesized with n = 6–8 and m = 6, 8, 10. The branched hydrophobic part of the surfactants introduces a large cross-section of the lipophilic surfactant moiety that is directly reflected in the shape of the micelles and the LC phase behavior in aqueous solution. The phase behavior of these V-amphiphiles is investigated with polarizing microscopy and x-ray diffraction and reveals that the branched lipophilic part strongly stabilizes the lamellar mesophase. This is in agreement with established packing models.

Key words: Non-ionic surfactant – oligo-oxyethylene surfactant – lyotropic liquid crystals – phase behavior

1. Introduction

In aqueous media the amphiphilic character of surfactant molecules leads to self organization into micelles and liquid-crystalline (LC) phases. The amphiphile organization in micelles results from the hydrophobic effect [1], which reduces the unfavorable contact of the hydrocarbon chains with water. The shape and size of the micelles are determined from the various geometric packing constraints of polar and apolar moieties of the amphiphiles. Consequently, the packing effect depends mainly on the chemical constitution of the amphiphile, the temperature, and the concentration in aqueous solution.

According to the simple geometrical model of Israelachvili [2] the surface area A at the interface, the volume V_l and the critical chain length l_c of the hydrocarbon chain strongly affect the micellar geometry. The critical packing parameter F,

$$F = V_l/l_c \cdot A \quad (1)$$

predicts the preferred micellar geometry. Above the critical micelle concentration (CMC) for $0 < F \leq 1/3$ spherical micelles, for $1/3 < F \leq 1/2$ cylindrical micelles, for $1/2 < F \leq 1$ disc-like micelles, and for $F > 1$ inverse micelles are predicted. Modifications of V_l/l_c or A are directly reflected in the shape of the micelles and the LC phase structure.

In a previous paper [3], we presented a concept for analyzing pure packing effects on the micellar shape and the LC phase structures of amphiphiles. It was suggested to modify the molecular architecture without affecting the hydrophilic-lipophilic balance (HLB) by introducing branched hydrophilic or hydrophobic moieties in oligo-oxyethylene alkyl ether amphiphiles depicted in Fig. 1. The different molecular geometries restrict the feasible packing arrangements and lead to different shapes of micelles and LC phase structures in water. By branching the hydrophilic chain in Y-amphiphiles (e.g., $C_nG(E_mM)_2$, where C_n denotes an alkyl chain, G a triglyceryl and E_mM an oligo-oxyethylene mono-methyl ether) a large

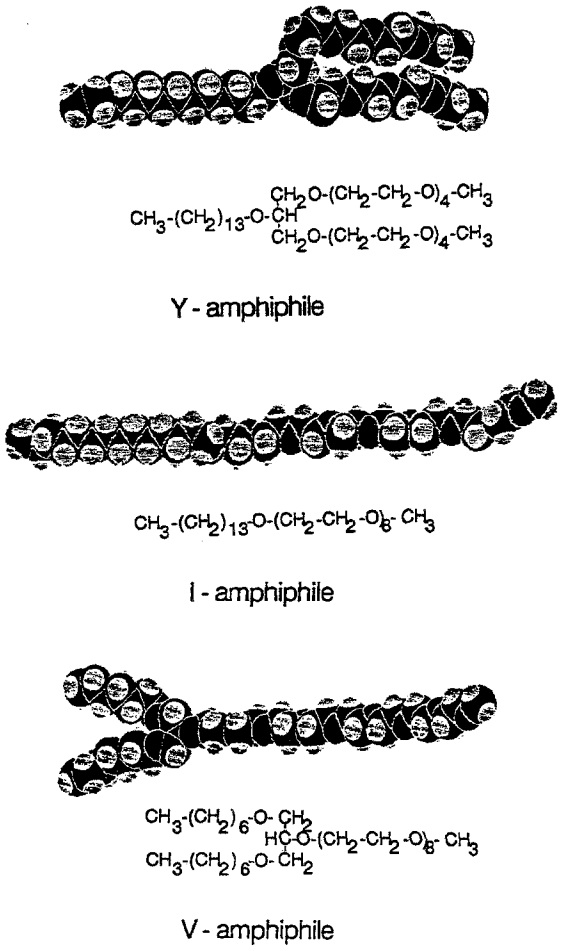

Fig. 1. Molecular models of corresponding Y-amphiphile $C_{14}G(E_4M)_2$; I-amphiphile $C_{14}E_8M$, and V-amphiphile $(C_7)_2GE_8M$ in extended conformation

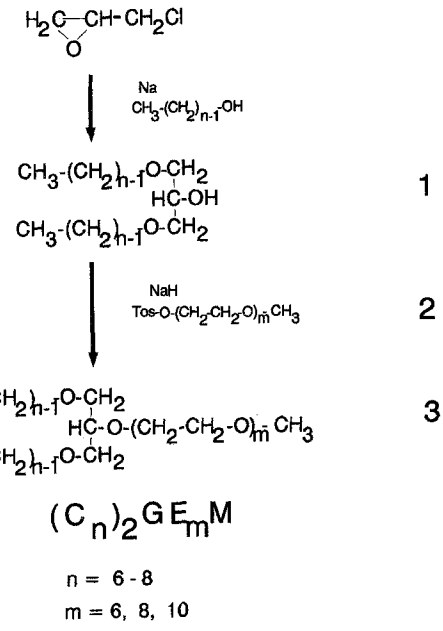

Scheme 1. Synthesis of $(C_n)_2GE_mM$ surfactants

interfacial area A per molecule at the micellar interface was realized. This causes a smaller critical packing parameter F than for the corresponding linear C_nE_mM I-amphiphiles. As a consequence spherical micelles and the stabilization of I_1 cubic phases were observed.

In this paper, we present new V-amphiphiles. These amphiphiles are modified at the hydrophobic groups by two alkyl chains. This causes an increase of the V_l/l_c ratio compared to the corresponding linear I-amphiphiles. The molecular model of such a V-amphiphile and a corresponding Y- and linear I-amphiphile is shown in Fig. 1. In addition to the synthesis of a homologous series of V-amphiphiles $(C_n)_2GE_mM$, the phase behavior of the new surfactants will be described with respect to the polymorphism of the lyotropic LC phases in aqueous solution. An explanation of the phase behavior of the homologous series of V-amphiphiles will be discussed, where the oxyethylene chain and alkyl chains are systematically modified. The LC phase polymorphism of V-amphiphiles is compared to the corresponding Y- and I-amphiphiles.

2. Experimental part

2.1. Synthesis

The V-amphiphiles $(C_n)_2GE_mM$ *3a–e* are synthesized according to standard procedures. In Scheme 1 the route for the synthesis of *3a–e* is presented. In the first reaction step, the sodium salt of the *n*-alkyl alcohol ($n = 6$–8) is treated with 1-chloro-2,3-epoxypropane yielding the glycerol dialkyl ether *1a–c* (refer to Table 1). In the second step the remaining free hydroxyl group is converted via sodium hydride into the sodium salt and etherified with the monodisperse tosylate *2* of the oligo-oxyethylene monomethyl ether ($m = 6, 8, 10$) to give the V-amphiphiles *3a–e* as colourless fluids in a yield of 35–55%.

Table 1. Properties, analytical data and yields of *1a–c*

1	*n*	$(C_n)_2GH$	mol. wt.	b °C/1 mbar	Yield %	Analysis found (calculated)	
						C/%	H/%
a	6	$C_{15}H_{32}O_3$	260.4	79–107	40	69.58(69.19)	12.57(12.39)
b	7	$C_{17}H_{36}O_3$	288.4	110–116	50	70.71(70.79)	12.75(12.58)
c	8	$C_{19}H_{40}O_3$	316.5	120–125	43	72.97(72.39)	12.85(12.76)

Table 2. Analytical data and yields of *3a–e*

3	*n*	*m*	$(C_n)_2GE_mM$	mol.wt.	Yield %	Analysis found (calculated)	
						C/%	H/%
a	6	8	$C_{32}H_{66}O_{11}$	626.8	42	61.41(61.32)	10.61(10.61)
b	7	8	$C_{34}H_{70}O_{11}$	645.8	53	62.13(62.36)	10.88(10.77)
c	8	8	$C_{36}H_{74}O_{11}$	682.9	41	63.31(63.32)	10.97(10.92)
d	7	10	$C_{38}H_{78}O_{13}$	742.8	34	61.34(61.42)	10.81(10.58)
e	7	6	$C_{30}H_{62}O_9$	566.8	40	63.43(63.57)	11.09(11.05)

2.1.1. Preparation of 1,3-bis-(n-alkyloxy)-2-propanol with n = 6–8 (1a–c)

0.6 mol *n*-alkyl alcohol is added dropwise to 0.25 mol of sodium hydride in 10 ml dry dioxane under nitrogen atmosphere. After stirring for 2 h at 65 °C, 0.2 mol 1-chloro-2,3-epoxypropane is slowly added at 40 °C. The mixture is stirred under reflux for 4 h and then at room temperature for 12 h. Thereafter the reaction mixture is concentrated. After addition of some water the organic layer is separated. The aqueous phase is acidified and extracted with ether. The combined organic phases are dried over sodium sulphate. The ether is evaporated and the residue is distilled under vacuum using a 30 cm Vigreux column to yield a colorless, clear liquid. The properties and analytical data for *1a–c* are shown in Table 1.
IR (film; cm^{-1}): 3560, 3440 (O–H); 2930, 2840 (C–H); 1450, 1370, 1250, 1100 (C–H, C–O, C–O–C).
^{1}H-NMR (80 MHz; $CDCl_3$/TMS; ppm): 0.9 (t, CH_3); 1.3 (m, CH_2); 2.3–2.4 (s, OH); 3.4 (m, OCH_2–G); 3.9 (m, OCH).

2.1.2. Preparation of methoxy-oligo-oxyethylenyl p-toluene sulfonate with m = 6, 8, 10 (2)

A mixture of 50 mmol p-toluenesulfonyl chloride, 25 mmol oligo-oxyethylene monomethyl ether ($m = 6, 8, 10$) and 100 ml dry diethyl ether is cooled under nitrogen atmosphere to − 20 °C. 250 mmol freshly powdered KOH is added over a period of 30 min to the cooled mixture. After stirring for 40–60 min, the reaction mixture is poured into ice water and the organic phase is separated. The aqueous phase is extracted once with diethyl ether and three times with methylene chloride. The collected CH_2Cl_2 extracts are dried over sodium sulphate. The solvent is removed under reduced pressure. The products are viscous, slightly yellow oils. Yield: 60–72% of *2*.
IR (film; cm^{-1}): 3040 (Bzl-H); 2860, 2800 (C–H); 1590 (C = C arom.); 1440, 1340 (C–H); 1285, 1240, 1175 (C–H, C–O); 1100 (C–O–C).
^{1}H-NMR (80 MHz, $CDCl_3$/TMS; ppm): 2.5 (s, Bzl–CH_3); 3.2 (s, OCH_3); 3.6 (m, OCH_2); 4.2 (t, J = 5Hz, CH_2-tos); 7.3 (d, J = 8Hz, Bzl-H_a); 7.8 (d, J = 8Hz, Bzl-H_b).

2.1.3. Preparation of 1,3-bis-(n-alkyloxy)-2-propoxy-m-oxyethylene monomethyl ether with n = 6–8 and m = 6, 8, 10 (3a–e)

7.5 mmol of *1* are added dropwise to 7.5 mmol sodium hydride in 10 ml dry diethyl ether at room temperature under nitrogen atmosphere. The mixture is stirred for 20 h at about 30 °C. Then 7.5 mmol of *2* are added dropwise. The mixture is

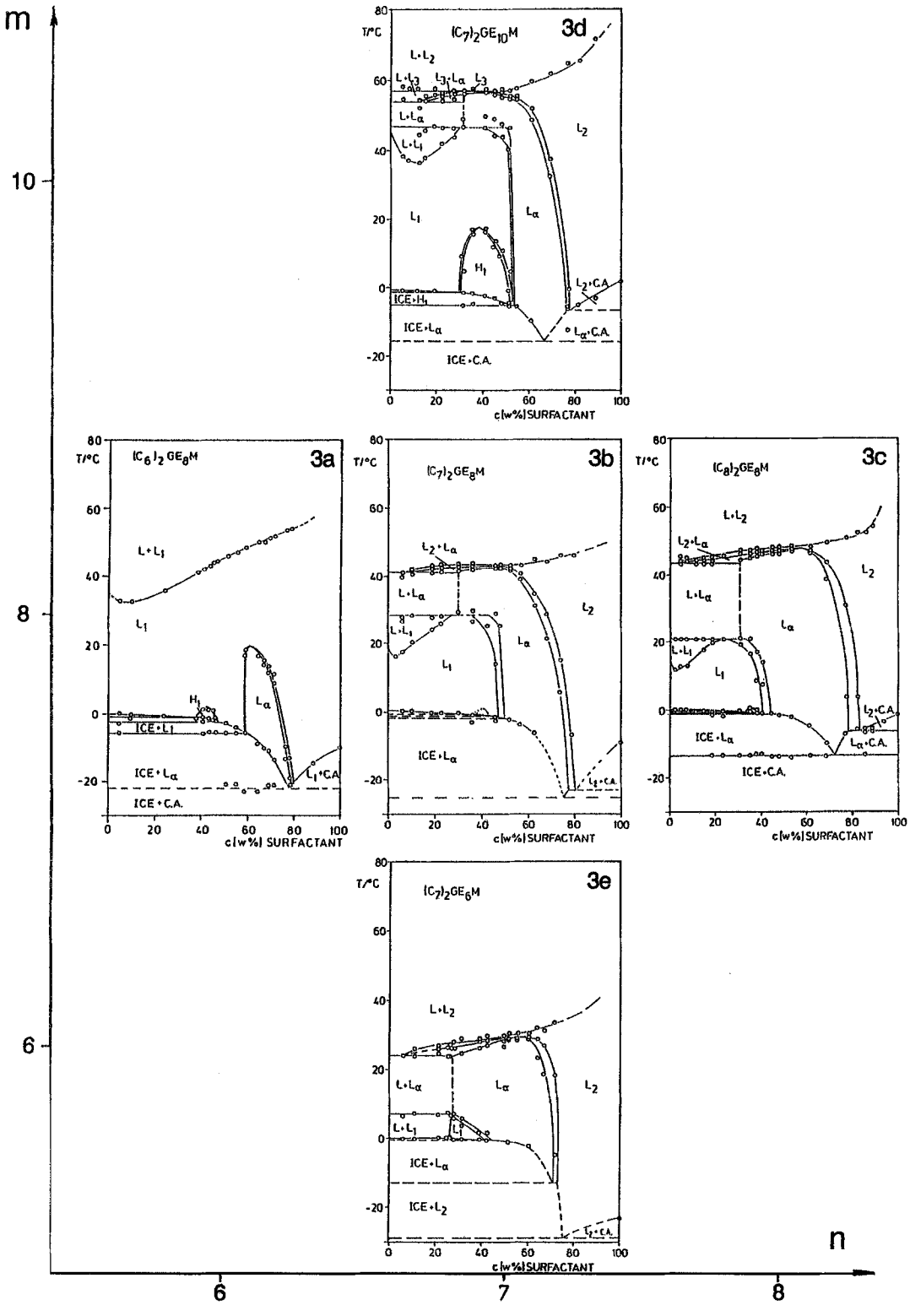

Fig. 2. Binary phase diagrams of $(C_n)_2GE_mM$ and water. The dependence of the phase behavior on alkyl chain length *n* and the number of oxyethylene units *m* per surfactant

heated to about 40 °C for 2 h. A white precipitate of sodium p-toluene sulfonate is filtered off and the product *3* is purified by flash chromatography with a diethyl ether/aceton (5/3 V/V) mixture as eluent. All products are colorless, viscous oils. The analytical data for *3a–e* are shown in Table 2.
IR (film; cm^{-1}): 2930, 2900, 2840, 1450, 1340 (C–H); 1300–1100 (C–O–C).
^{1}H-NMR (80 MHz, $CDCl_3$/TMS; ppm): 0.9 (t, CH_3); 1.3 (m, CH_2); 3.4 (s, OCH_3); 3.5–3.6 (m, OCH_2, OCH).

2.2. Measurements

2.2.1. Optical microscopy

All microscopic investigations are carried out with a Leitz-Ortholux II Pol-BK microscope equipped with a modified Mettler FP 80/82 hotstage which can be cooled with liquid nitrogen to − 60 °C. Samples of different concentrations are prepared using an analytical balance and mixed in Teflon capsules on a vibrating mill. All points of the phase transitions in the phase diagram are determined by heating the samples. Penetration technique experiments are performed to obtain a first information about the phase behavior, all temperature minima and maxima of the liquid crystalline and solid phases, and the eutectic and melting point.

2.2.2. X-ray diffraction

Diffraction studies are performed with a rotating anode generator (6.4 KW) in a point-collimated Kiesig camera under vacuum with Ni filtered CuKα radiation (λ = 1.542 Å) at distances of 390 mm. The samples are encapsulated in special thin-walled capillary glass tubes (2.0 mm diameter) and placed in a temperature-controlled sample holder. The exposure time takes about 23 h.

3. Results

3.1. Phase behavior

The phase behavior of the amphiphiles *3a–e* is determined over the whole concentration range in aqueous solution. The phase diagrams are shown in Fig. 2. It should be noted that the phase

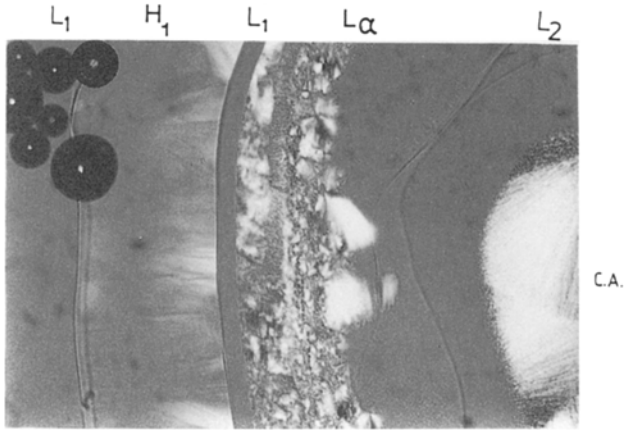

Fig. 3. Water penetration into *3d* showing from left to right: micellar phase L_1/hexagonal phase H_1/L_1/lamellar phase L_α/isotropic phase L_2/C.A. at 0.5 °C

sequence and the LC polymorphism of the surfactants is very similar. In these diagrams we can identify phase regions corresponding to the lamellar L_α, hexagonal H_1 phase and isotropic liquid phases such L_1, L_2, and L_3. For example, Fig. 3 shows a photograph of the contact preparation of *3d* surfactant with water. The phase boundary lines of H_1 and L_α phase can be recognized clearly. Characteristic data of *3a-e* are summarized in Table 3.

If we analyze the phase diagrams in detail, within this series of surfactants the following common behavior is observed in aqueous solution. Except for amphiphile *3e*, the amphiphiles *3a–d* are soluble over the whole concentration range and exhibit beside the isotropic solution L_1 and L_2 liquid crystalline phases. At low temperatures the solubility is limited by the crystallization of one component of the system and at high temperatures by a miscibility gap with a lower critical consolute point at the critical temperature T_c. The miscibility gap is strongly shifted unsymmetrically towards the water-rich side of the phase diagram. Above the cloud curve two isotropic solutions $L + L_1$ coexist. For *3e* the miscibility gap extends to temperatures as low as the liquidus line. For amphiphiles *3b–e* the cloud curve reaches the coexistence regime of the lamellar phase and the isotropic phase L_1. Above this temperature the biphasic regime of the miscibility gap consists of isotropic solution L and anisotropic L_α. The analysis of the phase boundary line between the

Table 3. Selected physical data for *3a–e* surfactants (T_{max} = maximum transition temperature of LC phase; T_c = lower critical consolute temperature; F = melting temperatrue of pure surfactant. Temperature in °C ± 0.5 °C)

Surfactant		LC phases H_1	T_{max} L_α	T_c	F
3a	$(C_6)_2GE_8M$	2.0	20.0	32.5	− 10.5
3b	$(C_7)_2GE_8M$	0.8	44.4	16.5	− 7.0
3c	$(C_8)_2GE_8M$	0.6	48.0	11.5	− 1.3
3d	$(C_7)_2GE_{10}M$	18.5	57.5	37.5	2.5
3e	$(C_7)_2GE_6M$	–	29.2	< 0	− 23.0

$L + L_\alpha$ biphasic regime and the homogeneous L_α phase is optically not well feasible and therefore indicated in the phase diagram with a dashed line.

At high amphiphile concentration all amphiphiles *3a–e* from lamellar L_α phase of low viscosity and with the characteristic optical textures of focal conic, mosaic, oily streaks and homeotropic areas. Additional to the microscopic texture, the lamellar phase is identified by x-ray measurements. Two diffraction rings in a ratio of 1:2 are observed; they correspond to the first- and second-order Bragg reflex resulting from the equally spaced layers of a lamellar phase.

Above the L_α phase of *3b–e* a narrow band of isotropic solution L_2 or L_3 is found. With increasing temperature these isotropic solutions separate into two coexisting isotropic solutions $L + L_2$ (miscibility gap).

Except for *3e* all investigated amphiphiles form at lower amphiphile concentration a highly viscous hexagonal H_1 phase. The existence domain for H_1 of *3a–c* is very small. For *3b* the H_1 phase is observed with a penetration experiment with the upper temperature limit of 0.8 °C. By thorough examination of samples of different concentrations the H_1 phase regime could not be found, so that the exact phase boundary lines are rather uncertain. In addition to the microscopic fan-shaped textures, the hexagonal phase is identified by x-ray measurements of *3d* with Bragg reflexes at angles that correspond to $1:\sqrt{3}:2$ distances, typical of a hexagonal lattice. Between the H_1 and L_α phase of *3a–d* no V_1 phase is observed, but the micellar solution L_1 exists.

At low temperatures a two-phase region is located between the liquidus line and the eutectic line. At concentrations below the eutectic point pure water crystallizes in presence of the isotropic phase L_1 or mesophases. At concentrations above the eutectic point crystalline amphiphile coexists with mesophase or isotropic phase L_2.

4. Discussion

The phase diagrams of the V-amphiphiles reveal that the LC polymorphism of this series is clearly determined by the molecular geometry according to the packing model. In the following we will discuss the phase behavior of amphiphiles in aqueous solutions: i) within a homologous series of V-amphiphiles depending on the HLB; ii) of corresponding V-, Y-, I-amphiphiles with the same HLB but different molecular geometry, and iii) of the corresponding homologous series of V-, Y-, I-amphiphiles in dependence on the HLB and molecular geometry.

i) Phase behavior within a homologous series of V-amphiphiles in dependence of the HLB

Within the homologous series of V-amphiphiles *3a–e* the polymorphism of the LC phases is very similar and independent of the HLB. The phase diagrams exhibit regions corresponding to lamellar and hexagonal phases (except for *3e*). If we analyze the LC phase behavior some systematic trends of the phase stability are obtained by changing the hydrophilic $(m)_n$ or lipophilic $(n)_m$ chain lengths (changing the HLB).

For the phase regime of the hexagonal H_1 phase we see a decrease of the H_1 stability (decrease of the upper temperature limit T_H) as $(n)_m$ increases *3a–c* and increasing H_1 stability as $(m)_n$ increases *3b, 3d* (see Fig. 4). These trends are in accordance with the packing model. Lengthening of the alkyl chains with a constant hydrophilic

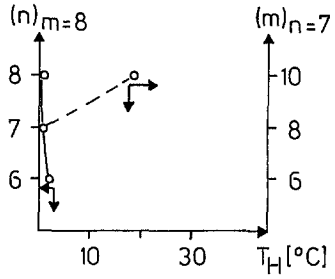

Fig. 4. Maximum transition temperature T_H of the H_1 phase depending on alkyl chain length n, and number of oxyethylene units m per surfactant

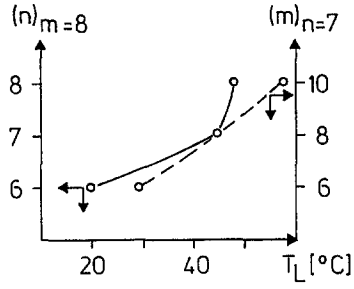

Fig. 5. Maximum transition temperature T_L of the L_α phase depending on alkyl chain length n, and number of oxyethylene units m per surfactant

group (A = const) leads to a larger lipophilic cross-section ratio V_1/l_c and therefore to a larger critical packing parameter F, which causes a destabilization of the hexagonal phase. The phase regime of the H_1 becomes smaller in favor of the lamellar L_α phase, as expected from Eq. (1). The lengthening of the oxyethylene chain with a constant lipophilic moiety (V_1/l_c = const) leads to a larger hydrophilic cross-section ratio A and therefore to a lower F parameter. The phase regime of the hexagonal phase enlarges.

For the phase regime of the lamellar L_α phase essentially the same arguments hold. It is interesting to note that an increase of the alkyl chains length $(n)_m$ by *3a–c* as well as an increase of the oligo-oxyethylene chain length $(m)_n$ by *3e, 3b, 3d* results in an increase of the upper temperature limit T_L for the lamellar phase (see Fig. 5). On the other hand, the concentration range of the lamellar phase becomes smaller with increasing $(m)_n$, but broadens significantly with increasing $(n)_m$.

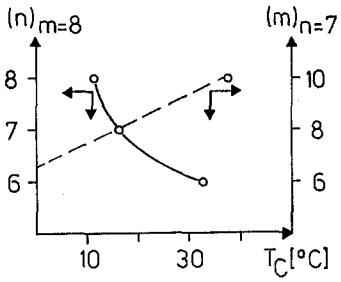

Fig. 6. Dependence of the cloud point T_c on alkyl chain length n, and number of oxyethylene units m per surfactant

Finally, the lower critical consolute temperatures T_c of the surfactant solution *3a–e* have to be mentioned. An elongation of the hydrophobic alkyl chains $(n)_m$ strongly reduces T_c. A shortening of the oxyethylene units $(m)_n$ also drastically reduces T_c (see Fig. 6).

ii) Phase behavior of V-, Y-, I-amphiphiles with the same HLB but different molecular geometry

The particular topological structure of the corresponding V-, Y- and I-amphiphiles is the dominant factor that determines the different phase behavior in water. The molecular geometry and especially the relative cross-section ratio of the polar and apolar surfactant moieties determine the packing arrangement (micellar shape) and the structure of the LC phase. For example, (see Fig. 7), the Y-amphiphile $C_{12}G(E_4M)_2$ [3] with the very large cross-section A of the polar moiety forms spherical micelles and cubic I_1 phases in water. Additionally, at high surfactant concentrations a small region of hexagonal H_1 phase is observed. The V-amphiphile *3a* with the same HLB, but a very large cross-section of the apolar moiety (V_1/l_c), shows a stabilization of the lamellar L_α phase. At low surfactant concentrations a small region of a hexagonal H_1 phase is observed. The corresponding linear I-amphiphile $C_{12}E_8M$ [4] shows a stabilization of the hexagonal H_1 phase and, additionally, a small region of cubic I_1 phases at lower surfactant concentrations. It should be mentioned, however, that within this series the HLB of the I-amphiphile slightly differs from the other systems.

For these surfactants the cross–section ratio of the polar and apolar surfactant moieties decreases

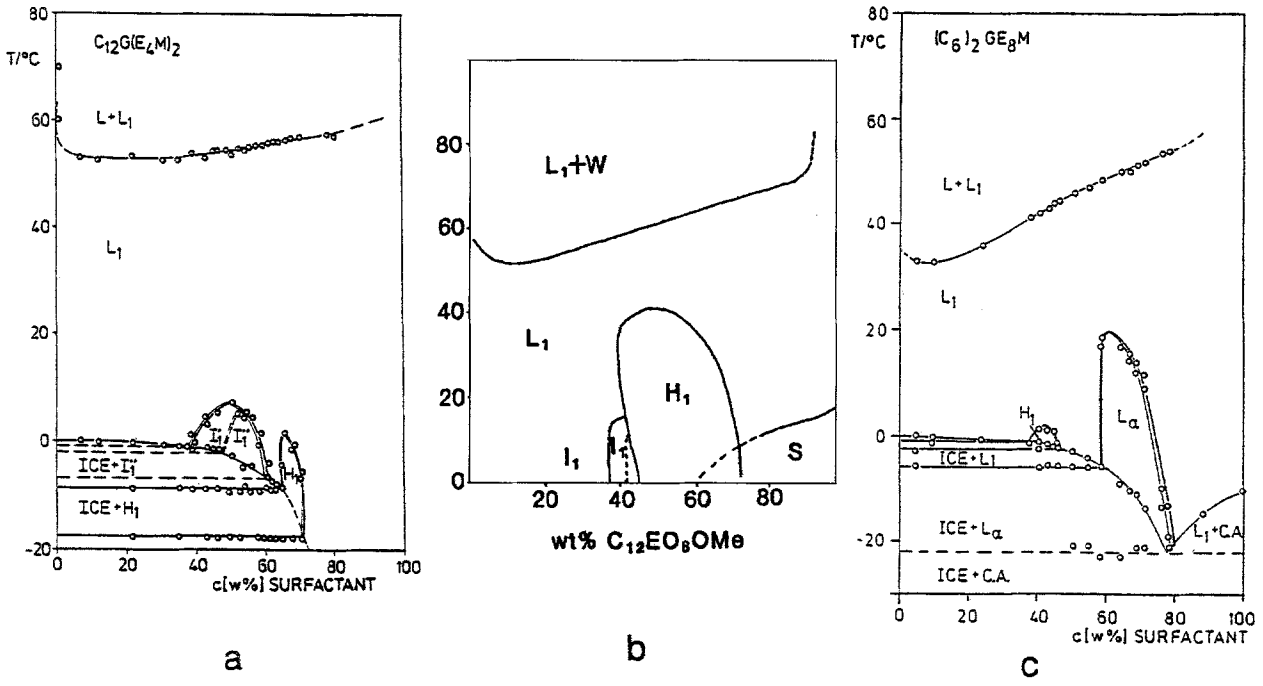

Fig. 7. Binary phase diagrams of corresponding amphiphiles with different molecular architecture (see Fig. 1) a) $C_{12}G(E_4M)_2$ (Y-amphiphile) [3]; b) $C_{12}E_8M$ (I-amphiphile) [4]; c) $(C_6)_2GE_8M$ (V-amphiphile)

in the series Y - I - V surfactants. As a consequence the curvature of the micellar associate decreases and a change of the dominant phase structure from cubic for Y-amphiphiles over hexagonal for I-amphiphiles to lamellar for *V*-amphiphiles is observed.

iii) Comparison of the phase behavior of the homologous series of V-,Y-,I-amphiphiles in dependence of HLB and molecular geometry

The influence of the molecular geometry on the phase behavior in water becomes evident if one considers the whole corresponding homologous series of V-, Y- and I-amphiphiles by variation of HLB. The homologous series of V-amphiphiles shows the same LC polymorphism independent of HLB. It clearly reflects the influence of the molecular geometry due to the splitting of the alkyl chain (large V_l/l_c). The critical packing parameter F_V compared to the corresponding I- and Y-amphiphiles is large. This causes the stabilization of bilayered micelles and particularly the formation of the lamellar phase.

The polymorphism of the LC phases within the corresponding homologous series of Y-amphiphiles [3] is very different to that of the V-amphiphiles. The phase diagrams exhibit two cubic I_1 phases and one hexagonal phase and is similar for all Y-amphiphiles and independent of the HLB. The branching of the hydrophilic chain increases the interfacial area A per molecule at the micellar interface. This causes a critical packing parameter F_Y smaller than for the corresponding I- and V-amphiphiles. Consequently stabilization of spherical micelles and I_1 cubic phases is observed.

In contrast to the previous observations, the LC phase polymorphism of the homologous series of corresponding I-amphiphiles $C_{12}E_mM$ $m = 4, 6, 8$ [4] is very different and strongly dependent on the HLB. The elongation of the hydrophilic chain leads to extreme changes in the LC phase structure (from L_α for $C_{12}E_4M$ to I_1/H_1 for $C_{12}E_8M$). This reflects the strong influence of the relative cross-section ratio of the polar and apolar surfactant moieties on the lengthening of polar chain due to the particular topological structure of the linear amphiphile.

It is interesting to note that the phase behavior of the homologous V-amphiphiles *3a–e* is very similar to the phase behavior of the homologous series of linear I-amphiphiles C_nE_m with $(n)_{m=4} = 10, 12$ and $(m)_{n=12} = 3–5$ [5]. The HLB of these homologous V- and I-amphiphiles is very different. This indicates that in accordance with the critical packing parameter model, the relative cross-section ratio of the polar (A) and apolar (V_1/l_c) surfactant moieties of these V- and I-amphiphiles must be alike.

Finally, we will compare the solubility and the lower critical consolute temperature T_c of the homologous series of V- and Y-amphiphiles. In general, the solubility and the miscibility gap of V-amphiphiles compared to the corresponding Y-amphiphiles is very different and strongly dependent on the HLB. The reason for the different solubility might be found in the different shape of micellar associates of these surfactants, which leads to different clouding process. The Y-amphiphiles form very stable, small, spherical micelles [6]. The size of the spherical micelles is determined by the chemical structure of the surfactant and cannot grow. Therefore, the clouding process mainly arises from the dehydration of the oxyethylene groups. This explains the nearly constant T_c (54.2–52.4 °C) of the homologous series of Y-amphiphiles $C_nG(E_4M)_2$ for $n = 10–16$ with the same hydrophilic moiety [3]. The V-amphiphiles probably form rods or disc-like micelles and the micellar growth has a larger influence on the clouding process than dehydration of oxyethylene groups with increasing temperature [4]. This argument is confirmed for the amphiphiles *3a–c* having the same hydrophilic moiety. The critical consolute temperatures T_c is lowered by 21 °C by lengthening of the lipophilic alkyl chains from $n = 6$ to $n = 8$. Simultaneously, we observe with decreasing solubility and decreasing T_c a stabilization of the lamellar phase.

5. Conclusions

To elucidate pure packing effects on the micellar shape and the formation of LC phases, a comparison between the phase behavior of Y-, I- and V-amphiphiles with similar HLB but different geometric relations between the polar and apolar surfactant moieties has been performed. It can be clearly noted that the LC phase behavior is essentially determined by the molecular geometry rather than by the HLB. Only in the I-amphiphile series is the LC polymorphism determined by the HLB.

While the molecular geometry of the surfactants clearly determines the LC polymorphism, the micellar shape in the isotropic phase region is still an open question. Although we know that the Y-amphiphiles form small spherical micelles, the micellar geometry of the V-amphiphiles with concentration and temperature still has to be analyzed. These measurements will clarify whether the systematics found for the LC phase regime also hold in isotropic solution with respect to the relation micellar shape and molecular geometry.

References

1. Tenford C (1980) The Hydrophobic Effect, 2nd End, John Wiley-Interscience, New York pp 51
2. Israelachvili JN, Mitchell DJ, Ninham BN (1976) J Chem Soc Faraday Trans 2, 72:1525
3. Kratzat K, Finkelmann H (1993) Liquid Crystal 13 (5):691
4. Conroy JP, Hall C, Leng CA, Rendall K, Tiddy GJT, Walsh J, Lindblom G (1990) Prog Colloid Polym Sci 82:253
5. Mitchell DJ, Tiddy GJT, Waring L, Bostock T, McDonald MP (1983) J Chem Soc Faraday Trans 1, 79:975
6. Berend K, Kratzat K, Burchard W (in press)

Received May 7, 1993
accepted August 4, 1993

Authors' address:

Krystyna Kratzat
Institut für Makromolekulare Chemie
Universität Freiburg
Stefan-Meier-Straße 31
79104 Freiburg i. Br., FRG